

# Peak Energy–Isotropic Energy Relation in the Off-Axis Gamma-Ray Burst Model

Ryo Yamazaki<sup>1</sup>, Kunihito Ioka<sup>2</sup>, and Takashi Nakamura<sup>1</sup>

yamazaki@tap.scphys.kyoto-u.ac.jp, ioka@vega.ess.sci.osaka-u.ac.jp,  
takashi@tap.scphys.kyoto-u.ac.jp

## ABSTRACT

Using a simple uniform jet model of prompt emissions of gamma-ray bursts (GRBs), we reproduce the observed peak energy–isotropic energy relation. A Monte Carlo simulation shows that the low-isotropic energy part of the relation is dominated by events viewed from off-axis directions, and the number of the off-axis events is about one third of the on-axis emissions. We also compute the observed event rates of the GRBs, the X-ray rich GRBs, and the X-ray flashes detected by *HETE-2*, and find that they are similar.

*Subject headings:* gamma rays: bursts —gamma rays: theory

## 1. Introduction

There is a strong correlation between the rest-frame spectral peak energy  $(1+z)E_p$  and the isotropic equivalent  $\gamma$ -ray energy  $E_{\text{iso}}$  of the gamma-ray bursts (GRBs). This relation ( $E_p$ – $E_{\text{iso}}$  relation) was first discovered by Amati et al. (2002), and recently extended down to lower energies (Atteia 2003; Lamb et al. 2003b; Sakamoto et al. 2003), so that  $E_{\text{iso}}$  ranges over five orders of magnitude. A similar relation, the  $E_p$ –luminosity relation is also found by Yonetoku et al. (2003), and both relations could become a new distance indicator. The geometrically corrected  $\gamma$ -ray energies  $E_\gamma = (1 - \cos \Delta\theta)E_{\text{iso}}$  narrowly cluster around a standard energy  $E_\gamma \sim 10^{51}$  ergs (Bloom, Frail, & Kulkarni 2003a; Frail et al. 2001), so that the opening half-angle of the jet in the on-axis uniform jet model ranges two and half orders of magnitude. This means that if the low isotropic energy events correspond to the wide opening half-angle jet, the jet opening half-angle of the typical GRBs  $\Delta\theta$  becomes less than

---

<sup>1</sup>Department of Physics, Kyoto University, Kyoto 606-8502, Japan

<sup>2</sup>Department of Earth and Space Science, Osaka University Toyonaka 560-0043, Japan

$1^\circ$  (Lamb, Donaghy, & Graziani 2003a). However such a small angle jet has difficulties in the standard afterglow models and observations. (see also Zhang & Mészáros 2003).

The low-energy (low- $E_p$ ) part of the relation consists of X-ray flashes (XRFs), that were identified by *BeppoSAX* (Heise et al. 2001) and other satellites (Gotthelf et al. 1996; Hamilton et al. 1996; Arefiev, Priedhorsky, & Borozdin 2003) and have been accumulated by *HETE-2* (Barraud et al. 2003). Theoretical models of the XRF have been widely discussed (Yamazaki, Ioka, & Nakamura 2003b): *high-redshift GRBs* (Heise et al. 2001; Barraud et al. 2003), *wide opening angle jets* (Lamb, Donaghy, & Graziani 2003a), *clean fireballs* (Mochkovitch et al. 2003; Daigne & Mochkovitch 2003), *failed GRBs or dirty fireballs* (Dermer et al. 1999; Huang, Dai, & Lu 2002; Dermer & Mitman 2003), *photosphere-dominated fireballs* (Mészáros et al. 2002; Ramirez-Ruiz & Lloyd-Ronning 2002; Drenkhahn & Spruit 2002), *peripheral emissions from collapsar jets* (Zhang, Woosley, & Heger 2003) and *off-axis cannonballs* (Dar & De Rújula 2003). The issue is what is the main population among them.

We have already proposed *the off-axis jet model* (Yamazaki, Ioka, & Nakamura 2002, 2003b). The viewing angle is the key parameter to understand the various properties of the GRBs and may cause various relations such as the luminosity-variability/lag relation, the  $E_p$ -luminosity relation and the luminosity-width relation (Ioka & Nakamura 2001; Salmonson & Galama 2002). When the jet is observed from off-axis, it looks like an XRF because of the weaker blue-shift than the GRB.

There are some criticisms against our off-axis jet model. The original version of our model (Yamazaki, Ioka, & Nakamura 2002) required the source redshift less than  $\sim 0.4$  to be bright enough for detection, conflicting with the observational implications (e.g., Heise 2002; Bloom et al. 2003b). Yamazaki, Ioka, & Nakamura (2003b) showed that higher redshifts ( $z \gtrsim 1$ ) are possible with narrowly collimated jets ( $\lesssim 0.03$  rad), while such small jets have not yet been inferred by afterglow observations (Bloom, Frail, & Kulkarni 2003a; Panaiteescu & Kumar 2002; Frail et al. 2001). The luminosity distance to the sources at  $z \sim 0.4$  is  $d_L \sim 2$  Gpc, that is only a factor 3 smaller than that at  $z \sim 1$  (corresponding to  $d_L \sim 7$  Gpc). Thus small changes of parameters in our model allow us to extend the maximum redshift of the off-axis jets to  $z \gtrsim 1$  even for  $\Delta\theta \sim 0.1$ . This will be explicitly shown in § 3. Therefore, off-axis events may represent a large portion of whole observed GRBs and XRFs since the solid angle to which the off-axis events are observed is large.

In this paper, taking into account the viewing angle effects, we derive the observed  $E_p$ - $E_{\text{iso}}$  relation in our simple uniform jet model. This paper is organized as follows. In § 2 we describe a simple off-axis jet model for the XRFs. Then, in § 3, it is shown that the off-axis emission from the cosmological sources can be observed, and the  $E_p$ - $E_{\text{iso}}$  relation is discussed in § 4. Section 5 is devoted to discussions. We also show that the observed event

rates of GRBs and XRFs are reproduced in our model. Throughout the paper we adopt a  $\Lambda$ CDM cosmology with  $(\Omega_m, \Omega_\Lambda, h) = (0.3, 0.7, 0.7)$ .

## 2. Prompt emission model of GRBs

We use a simple jet model of prompt emission of GRBs considered in our previous works (Yamazaki, Ioka, & Nakamura 2003b; Yamazaki, Yonetoku, & Nakamura 2003). Note that the cosmological effect is included in these works (see also Yamazaki, Ioka, & Nakamura 2002, 2003a; Ioka & Nakamura 2001). We adopt an instantaneous emission, at  $t = t_0$  and  $r = r_0$ , of an infinitesimally thin shell moving with the Lorentz factor  $\gamma$ . Then the observed flux of a single pulse at frequency  $\nu = \nu_z/(1+z)$  and time  $T$  is given by

$$F_\nu(T) = \frac{2(1+z)r_0cA_0}{d_L^2} \frac{\Delta\phi(T)f[\nu_z\gamma(1-\beta\cos\theta(T))]}{[\gamma(1-\beta\cos\theta(T))]^2}, \quad (1)$$

where  $1-\beta\cos\theta(T) = (1+z)^{-1}(c\beta/r_0)(T-T_0)$  and  $A_0$  determines the normalization of the emissivity. The detailed derivation of equation (1) and the definition of  $\Delta\phi(T)$  are found in Yamazaki et al. (2003b). In order to have a spectral shape similar to the observed one (Band et al. 1993), we adopt the following form of the spectrum in the comoving frame,

$$f(\nu') = \begin{cases} (\nu'/\nu'_0)^{1+\alpha_B} \exp(-\nu'/\nu'_0) & \text{for } \nu'/\nu'_0 \leq \alpha_B - \beta_B \\ (\nu'/\nu'_0)^{1+\beta_B} (\alpha_B - \beta_B)^{\alpha_B - \beta_B} \exp(\beta_B - \alpha_B) & \text{for } \nu'/\nu'_0 \geq \alpha_B - \beta_B \end{cases}, \quad (2)$$

where  $\nu'_0$ ,  $\alpha_B$ , and  $\beta_B$  are the break energy, the low- and high- energy photon index, respectively. Equations (1) and (2) are the basic equations to calculate the flux of a single pulse. The observed flux depends on nine parameters:  $\gamma$ ,  $\alpha_B$ ,  $\beta_B$ ,  $\Delta\theta$ ,  $A_0\gamma^4$ ,  $r_0/\beta c\gamma^2$ ,  $\gamma\nu'_0$ ,  $z$ , and  $\theta_v$ .

## 3. The Maximum Distance of the Observable *BeppoSAX-XRFs*

In this section, we calculate the observed peak flux and the photon index in the energy band 2–25 keV as a function of the viewing angle  $\gamma\theta_v$ . The adopted parameters are  $\Delta\theta = 0.1$ ,  $\alpha_B = -1$ ,  $\beta_B = -2.5$ ,  $\gamma\nu'_0 = 300$  keV and  $r_0/\beta c\gamma^2 = 10$  s (Preece et al. 2000). We fix the amplitude  $A_0\gamma^4$  so that the isotropic equivalent  $\gamma$ -ray energy  $E_{\text{iso}} = 4\pi d_L^2(1+z)^{-1}S(20\text{--}2000\text{ keV})$  satisfies the condition

$$\frac{1}{2}(\Delta\theta)^2 E_{\text{iso}} = E_\gamma \text{ (} = \text{const.} \text{)} , \quad (3)$$

when  $\theta_v = 0$ . In this section, we take the standard energy constant  $E_\gamma = 1.15 \times 10^{51}$  ergs (Bloom, Frail, & Kulkarni 2003a). Then we obtain  $\gamma^4 A_0 = 2.6 \times 10^8$  erg cm $^{-2}$ . The redshift is varied from  $z = 0.01$  to  $1.0$ .

For our newly adopted parameters and the spectral function in equation (2), we draw the revised version of Fig. 3 in Yamazaki, Ioka, & Nakamura (2002), which originally assumed a different functional form of  $f(\nu')$  and used the old parameters  $E_\gamma = 0.5 \times 10^{51}$  erg (Frail et al. 2001) and  $\beta_B = -3$ . Figure 1 shows the results. Although qualitative differences between old and new versions are small, large quantitative differences exist. Since we now take into account the cosmological effects which were entirely neglected in the previous version, the observed spectrum becomes softer at higher  $z$ . The dotted lines in Figure 1 connect the same values of  $\gamma\theta_v$  with different  $z$ . The observed XRFs take place up to  $z \sim 1$  in contrast to our previous result of  $z = 0.4$  and have viewing angles  $\Delta\theta \lesssim \theta_v \lesssim 2\Delta\theta$ . The reason for this difference comes from the increase of the jet energy, the different spectrum and the different high-energy photon index. It is interesting to note that the only known redshift for XRFs so far is  $z = 0.25$ , one of the nearest bursts ever detected (Sakamoto et al. 2003; Soderberg et al. 2003).

We roughly estimate the event rate of the XRF detected by WFC/*BeppoSAX* (Yamazaki, Ioka, & Nakamura 2002). From the above results, the jet emission with an opening half-angle  $\Delta\theta$  is observed as the XRF (GRB) when the viewing angle is within  $\Delta\theta \lesssim \theta_v \lesssim 2\Delta\theta$  ( $0 \lesssim \theta_v \lesssim \Delta\theta$ ). Therefore, the ratio of each solid angle is estimated as  $f_{\text{XRF}}/f_{\text{GRB}} \sim (2^2 - 1^2)/1^2 = 3$ . Using this value, we obtain  $R_{\text{XRF}} \sim 1 \times 10^3$  events yr $^{-1}$  for the distance to the farthest XRF  $d_{\text{XRF}} = 6$  Gpc (see equation (5) of Yamazaki, Ioka, & Nakamura 2002). The derived value is comparable to the observation, or might be an over estimation which may be reduced since the flux from the source located at  $d_{\text{XRF}} \sim 6$  Gpc is too low to be observed if the viewing angle  $\theta_v$  is as large as  $\sim 2\Delta\theta$ . The ratio of the event rates of GRBs, X-ray rich GRBs (XR-GRBs) and XRFs detected by *HETE-2* will be discussed in the following sections.

#### 4. $E_{\text{p}}-E_{\text{iso}}$ Relation of *HETE* Bursts

In this section, we perform Monte Carlo simulations to show that our off-axis jet model can derive the observed  $E_{\text{p}}-E_{\text{iso}}$  relation and the event rate of the XRFs, the XR-GRBs and the GRBs detected by *HETE-2*. We randomly generate  $10^4$  bursts, each of which has the observed flux given by equations (1) and (2). In order to calculate the observed spectrum and fluence from each burst, we need eight parameters:  $\gamma$ ,  $\alpha_B$ ,  $\beta_B$ ,  $\Delta\theta$ ,  $A_0\gamma^4(r_0/\beta c\gamma^2)^2$ ,  $\gamma\nu'_0$ ,  $z$ , and  $\theta_v$ . They are determined in the following procedure.

1. We fix  $\gamma = 100$ . The parameters  $\alpha_B$ ,  $\beta_B$ , and  $\Delta\theta$  are allowed to have the following distributions. The distribution of the low-energy (high-energy) photon index  $\alpha_B$  ( $\beta_B$ ) is assumed to be normal with an average of  $-1$  ( $-2.3$ ) and a standard deviation of  $0.3$  ( $0.3$ ) (Preece et al. 2000). The distribution of the opening half-angle of the jet,  $\Delta\theta$ , is fairly unknown. Here we assume a power-law form given as  $f_{\Delta\theta} d(\Delta\theta) \propto (\Delta\theta)^{-q} d(\Delta\theta)$  for  $\Delta\theta_{\min} < \Delta\theta < \Delta\theta_{\max}$ . We take  $q = 2$  for the fiducial case, and adopt  $\Delta\theta_{\max} = 0.3$  and  $\Delta\theta_{\min} = 0.03$  rad, which correspond to the maximum and minimum values inferred from observations, respectively (Frail et al. 2001; Panaiteescu & Kumar 2002; Bloom, Frail, & Kulkarni 2003a).
2. Secondly, we choose  $E_{\gamma}|_{z=0}^{\theta_v=0}$ , that is the geometrically-corrected  $\gamma$ -ray energy of the source in the case of  $z = 0$  and  $\theta_v = 0$ , according to the narrow log-normal distribution with an average and a standard deviation of  $51 + \log(1.15)$  and  $0.3$ , respectively, for  $\log(E_{\gamma}|_{z=0}^{\theta_v=0}/1 \text{ erg})$  (Bloom, Frail, & Kulkarni 2003a). Then, the isotropic equivalent  $\gamma$ -ray energy for  $z = 0$  and  $\theta_v = 0$  is calculated as  $E_{\text{iso}}|_{z=0}^{\theta_v=0} = 2(\Delta\theta)^{-2}E_{\gamma}|_{z=0}^{\theta_v=0}$  to determine the flux normalization  $A_0\gamma^4(r_0/\beta c\gamma^2)^2$ .
3. Thirdly, we assume the *intrinsic*  $E_{\text{p}}-E_{\text{iso}}$  relation for  $z = 0$  and  $\theta_v = 0$ :

$$E_{\text{p}}|_{z=0}^{\theta_v=0} = 100 \xi \text{ keV} \left( \frac{E_{\text{iso}}|_{z=0}^{\theta_v=0}}{10^{51} \text{ ergs}} \right)^{1/2}. \quad (4)$$

This may be a consequence of the standard synchrotron shock model (Zhang & Mészáros 2002b; Ioka & Nakamura 2002), but we do not discuss the origin of this intrinsic relation in this Letter. The coefficient  $\xi$  is assumed to obey the log-normal distribution (Ioka & Nakamura 2002), where an average and a standard deviation of  $\log \xi$  are set to  $-0.7$  and  $0.15$ , respectively. We determine  $\gamma\nu'_0$  such that the calculated spectrum  $\nu S_{\nu}$  has a peak energy  $E_{\text{p}}|_{z=0}^{\theta_v=0}$  when  $\theta_v = 0$  and  $z = 0$ .

4. Finally, we choose the source redshift  $z$  and the viewing angle  $\theta_v$  to calculate the observed spectrum and fluence, and find  $E_{\text{p}}$  and  $E_{\text{iso}}$ . The source redshift distribution is assumed to trace the cosmic star formation rate, and the probability distribution of  $\theta_v$  is  $P(\theta_v) d\theta_v \propto \sin \theta_v d\theta_v$ . To determine the redshift distribution, we assume the model SF2 of the star formation rate given by Porciani & Madau (2001).

We place a fluence truncation of  $5 \times 10^{-8} \text{ erg cm}^{-2}$  to reflect the limiting sensitivity of detectors on *HETE-2*. Although the detection conditions of instruments vary with many factors of each event (Band 2003), we consider a very simple criterion here. This fluence truncation condition is also adopted in Zhang & Mészáros (2003).

Figure 2 shows a result. Among  $10^4$  simulated events, 288 events are detected by *HETE-2*. The others cannot be observed because their viewing angles are so large that the relativistic beaming effect reduces their observed flux below the limiting sensitivity. Pluses (+) and crosses ( $\times$ ) represent bursts detected by *HETE-2*; the former corresponds to on-axis events ( $\theta_v < \Delta\theta$ ) while the latter to off-axis events ( $\theta_v > \Delta\theta$ ). The events denoted by dots are not detected. The numbers of on-axis and off-axis events are 209 and 79, respectively. Nearby events ( $z \lesssim 1$ ) with large viewing angles can be seen. Such bursts are mainly soft events with  $(1+z)E_p$  less than  $\sim 60$  keV.

When  $\theta_v < \Delta\theta$ ,  $E_p$  is related to  $E_{\text{iso}}$  as  $E_p \propto E_{\text{iso}}^{1/2}$  [see equation (4)]. The dispersion of pluses (+) in the  $E_p$ – $E_{\text{iso}}$  plane mainly comes from those of “intrinsic” quantities such as  $E_\gamma|_{z=0}^{\theta_v=0}$ ,  $\Delta\theta$  and  $\xi$ .

On the other hand, even when  $\theta_v > \Delta\theta$ , the relation  $E_p \propto E_{\text{iso}}^{1/2}$  is nearly satisfied for the observed sources. The reason is as follows. For a certain source, as the viewing angle increases, the relativistic beaming and Doppler effects reduce the observed fluence and peak energy, respectively. When the point source approximation is appropriate for the large- $\theta_v$  case, the isotropic energy and the peak energy depend on the Doppler factor  $\delta = [\gamma(1 - \beta \cos(\theta_v - \Delta\theta))]^{-1}$  as  $E_{\text{iso}} \propto S(20 - 2000 \text{ keV}) \propto \delta^{1-\langle\alpha\rangle}$  and  $E_p \propto \delta$ , respectively (Ioka & Nakamura 2001; Yamazaki, Ioka, & Nakamura 2002; Dar & De Rújula 2003). Hence we obtain  $E_{\text{iso}} \propto E_p^{1-\langle\alpha\rangle}$ . Here  $\langle\alpha\rangle$  is the mean photon index in the 20–2000 keV band, which ranges between  $\beta_B$  and  $\alpha_B$ . Therefore we can explain the relation  $E_p \propto E_{\text{iso}}^{1/2}$  for  $\langle\alpha\rangle \sim \alpha_B \sim -1$ . On the other hand, when  $\theta_v$  is large enough for  $E_p$  to be smaller than 20 keV, we find  $E_{\text{iso}} \propto E_p^{1-\beta_B} \sim E_p^{3.3}$  or  $E_p \propto E_{\text{iso}}^{0.3}$  since  $\langle\alpha\rangle \sim \beta_B$ . In this case, the relation deviates from the line  $E_p \propto E_{\text{iso}}^{1/2}$ , and the dispersion of  $E_{\text{iso}}$  becomes large for small  $E_p$ .

## 5. Discussion

We have shown that the observed  $E_p$ – $E_{\text{iso}}$  relation can be explained by our simple uniform jet model. The low-isotropic energy part of the relation is dominated by off-axis events. The number of the off-axis events is about one third of on-axis emissions. An important prediction of our model has been also derived, i.e., we will see the deviation from the present relation  $E_p \propto E_{\text{iso}}^{1/2}$  if the statistics of the low-energy bursts increase. *Swift* satellite will bring a new insight into this aspect by detecting a number of dim bursts.

*HETE*-team gives definitions of the XRF and the XR-GRB in terms of the hardness ratio: XRFs and XR-GRBs are events for which  $\log[S_X(2-30 \text{ keV})/S_\gamma(30-400 \text{ keV})] > 0.0$  and  $-0.5$ , respectively (Lamb et al. 2003b; Sakamoto et al. 2003). We calculate the hardness

ratio for simulated bursts surviving the fluence truncation condition, and classify them into GRBs, XR-GRBs, and XRFs. It is then found that all XRFs have redshift smaller than 5. The ratio of the observed event rate becomes  $R_{GRB} : R_{XR-GRB} : R_{XRF} \sim 2 : 5 : 1$ . This ratio mainly depends on the value of  $q$ . When  $q$  becomes small, jets with large  $\Delta\theta$  increases, and hence intrinsically dim bursts (i.e., low- $E_{\text{iso}}|_{z=0}^{\theta_v=0}$  bursts) are enhanced. Owing to equation (4), soft events are enhanced. In the case of  $q = 1$  with the other parameters remaining fiducial values, the ratio is  $R_{GRB} : R_{XR-GRB} : R_{XRF} \sim 1 : 9 : 3$ . For any cases we have done, the number of XR-GRBs is larger than those of GRBs and XRFs, while the event rate of them are essentially comparable with each other. *HETE-2* observation shows  $R_{GRB} : R_{XR-GRB} : R_{XRF} \sim 1 : 1 : 1$  (Lamb et al. 2003b). Although possible instrumental biases may change the observed ratio (Suzuki, M. & Kawai, N., private communication), we need more studies in order to bridge a small gap between the theoretical and the observational results.

The  $E_{\text{p}}-E_{\text{iso}}$  diagram of the GRB population may be a counterpart of the Herzsprung-Russell diagram of the stellar evolution. The main sequence stars cluster around a single curve which is a one-parameter family of the stellar mass. This suggests that the  $E_{\text{p}}-E_{\text{iso}}$  relation of the GRB implies the existence of a certain parameter that controls the GRB nature like the stellar mass. We have shown that the viewing angle is one main factor to explain the  $E_{\text{p}}-E_{\text{iso}}$  relation kinematically. Our model predicts the deviation of this relation in the small  $E_{\text{iso}}$  region, which may be confirmed in future.

In the uniform jet model, the afterglows of off-axis jets should resemble the orphan afterglows that initially have a rising light curve (e.g., Yamazaki, Ioka, & Nakamura 2003a; Granot et al. 2002). This problem could be overcome by introducing a Gaussian tail around the uniform jet (Zhang & Mészáros 2003). Other possibilities to evade this problem will be presented elsewhere (Yamazaki, Ioka, & Nakamura 2004, in preparation).

We would like to thank G. R. Ricker, T. Murakami, N. Kawai, A. Yoshida, and M. Suzuki for useful comments and discussions. Numerical computation in this work was carried out at the Yukawa Institute Computer Facility. This work was supported in part by a Grant-in-Aid for the 21st Century COE “Center for Diversity and Universality in Physics” and also supported by Grant-in-Aid for Scientific Research of the Japanese Ministry of Education, Culture, Sports, Science and Technology, No.05008 (RY), No.660 (KI), No.14047212 (TN), and No.14204024 (TN).

## REFERENCES

Amati, L. et al. 2002, *A&A*, 390, 81

Arefiev, V. A., Priedhorsky, W. C., & Borozdin, K. N. 2003, *ApJ*, 586, 1238

Atteia, J.-L. 2003, *A&A*, 407, L1

Band, D. et al. 1993, *ApJ*, 413, 281

Band, D.L., 2003, *ApJ*, 588, 945

Barraud, C. et al. 2003, *A&A*, 400, 1021

Bloom, J. S., Frail, D. A., & Kulkarni, S. R. 2003a, *ApJ*, 594, 674

Bloom, J. S., Fox, D., van Dokkum, P. G., Kulkarni, S. R., Berger, E., Djorgovski, S. G., & Frail, D. A. 2003b, *ApJ*, 599, 957

Daigne, F. & Mochkovitch, R. 2003, *MNRAS*, 342, 587

Dar, A. & De Rújula, A. 2003, *astro-ph/0309294*

Dermer, C. D., Chiang, J., & Böttcher, M. 1999, *ApJ*, 513, 656

Dermer, C. D. & Mitman, K. E. 2003, in proc. of Third Rome Workshop: Gamma-Ray Bursts in the Afterglow Era. (*astro-ph/0301340*)

Drenkhahn, G. & Spruit, H. C. 2002, *A&A*, 391, 1141

Frail, D. A. et al. 2001, *ApJ*, 562, L55

Gotthelf, E. V., Hamilton, T. T., & Helfand, D. J. 1996, *ApJ*, 466, 779

Granot, J., Panaitescu, A., Kumar, P., & Woosley, S. E. 2002, *ApJ*, 570, L61

Hamilton, T. T., Gotthelf, E. V., & Helfand, D. J. 1996, *ApJ*, 466, 795

Heise, J., in 't Zand, J., Kippen, R. M., & Woods, P. M. 2001, in Proc. Second Rome Workshop: Gamma-Ray Bursts in the Afterglow Era, ed. E. Costa, F. Frontera, & J. Hjorth (Berlin: Springer), 16 (*astro-ph/0111246*)

Heise, J. 2002, talk given in Third Rome Workshop: Gamma-Ray Bursts in the Afterglow Era.

Huang, Y. F., Dai, Z. G., & Lu, T. 2002, *MNRAS*, 332, 735

Ioka, K., & Nakamura, T. 2001, ApJ, 554, L163

Ioka, K., & Nakamura, T. 2002, ApJ, 570, L21

Lamb, D. Q., Donaghy, T. Q., & Graziani, C. 2003a, astro-ph/0312634

Lamb, D.Q. et al. 2003b, astro-ph/0309462

Mészáros, P., Ramirez-Ruiz, E., Rees, M. J., & Zhang, B. 2002, ApJ, 578, 812

Mochkovitch, R., Daigne, F., Barraud, C., & Atteia, J. 2003, astro-ph/0303289

Panaitescu, A. & Kumar, P. 2002, ApJ, 571, 779

Porciani, C. & Madau, P. 2001, ApJ, 548, 522

Preece, R. D., Briggs, M. S., Mallozzi, R. S., Pendleton, G. N., Paciesas, W. S., & Band, D. L. 2000, ApJS, 126, 19

Ramirez-Ruiz, E. & Lloyd-Ronning, N. M. 2002, New Astronomy, 7, 197

Sakamoto, T., et al. 2003, ApJ, in press (astro-ph/0309455)

Salmonson, J. D. & Galama, T. J. 2002, ApJ, 569, 682

Soderberg, A. M., et al. 2003, submitted to ApJ (astro-ph/0311050)

Yamazaki, R., Ioka, K., & Nakamura, T. 2002, ApJ, 571, L31

Yamazaki, R., Ioka, K., & Nakamura, T. 2003a, ApJ, 591, 283

Yamazaki, R., Ioka, K., & Nakamura, T. 2003b, ApJ, 593, 941

Yamazaki, R., Yonetoku, D., & Nakamura, T. 2003, ApJ, 594, L79

Yonetoku, D., et al. 2003, submitted to ApJL (astro-ph/0309217)

Zhang, B. & Mészáros, P. 2002b, ApJ, 581, 1236

Zhang, B. & Mészáros, P. 2003, astro-ph/0311190

Zhang, W., Woosley, S. E., & Heger, A. 2003, astro-ph/0308389

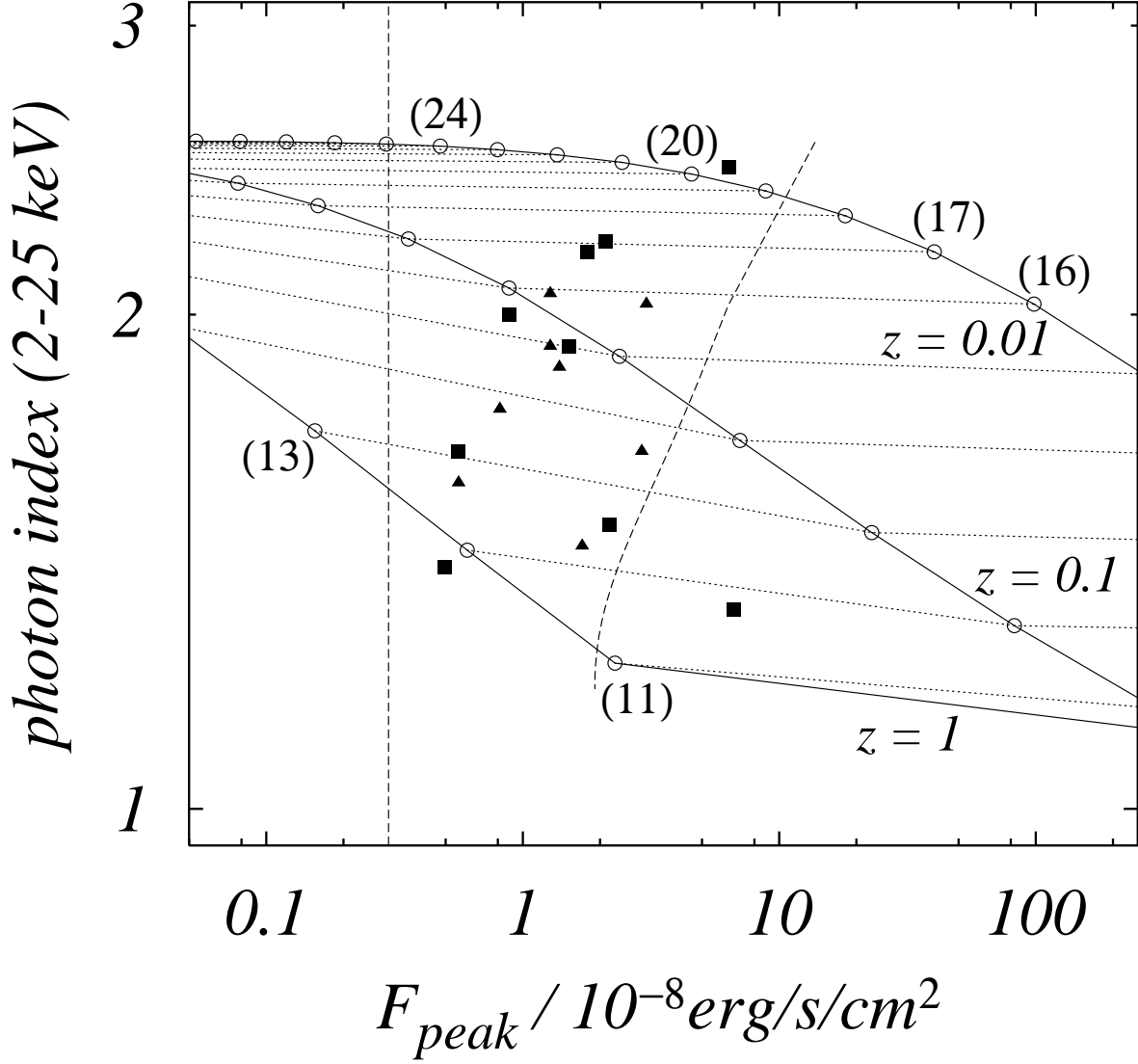


Fig. 1.— Photon index in the energy range 2–25 keV as a function of the peak flux in the same energy range by varying the source redshift  $z$ . This figure is the updated version of Fig. 3 in Yamazaki, Ioka, & Nakamura (2002). We adopt  $\gamma\Delta\theta = 10$ ,  $\alpha_B = -1$ ,  $\beta_B = -2.5$ , and  $\gamma\nu'_0 = 300$  keV. The values of the viewing angle  $\gamma\theta_v$  are given in parenthesis. Three solid curves correspond to  $z = 0.01$ ,  $0.1$ , and  $1$ , respectively. The same values of  $\gamma\theta_v$  with different  $z$  are connected by dotted lines. The observed data of *BeppoSAX*-XRFs are shown from Heise et al. (2001). Squares (triangles) are those which were (were not) detected by BATSE. Two dashed lines represent observational bounds. Note that an operational definition of the XRF detected by Wide Field Cameras (WFCs) on *BeppoSAX* is a fast X-ray transient that is not triggered and not detected by the Gamma-Ray Burst Monitor (GRBM) (Heise et al. 2001). In the region to the left of the vertical dashed line, the peak flux in the X-ray band is smaller than the limiting sensitivity of WFCs, and such events cannot be observed. In the region to the right of the oblique dashed line, the peak flux in the  $\gamma$ -ray band is larger than the limiting sensitivity of the GRBM, and such events are observed as GRBs.

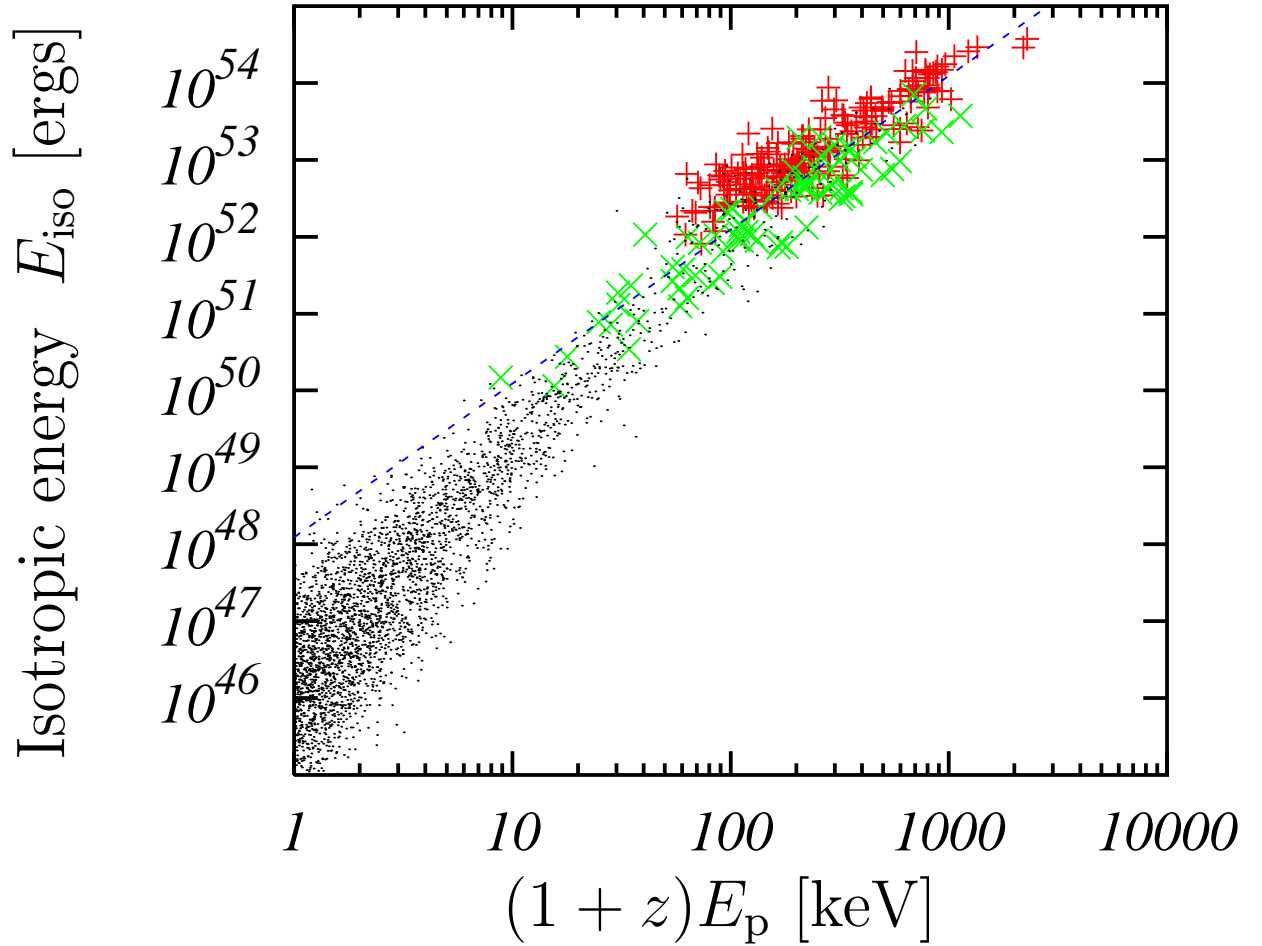


Fig. 2.— Distribution of simulated bursts in the  $(1 + z)E_p$ – $E_{\text{iso}}$  plane. Pluses (+) and crosses (x) represent bursts that can be detected by *HETE-2*; the former is on-axis events ( $\theta_v < \Delta\theta$ ) while the latter is the off-axis case ( $\theta_v > \Delta\theta$ ). The events denoted by dots are not detected. The dashed line represents the best fit of the observation given by  $E_p \sim 95$  keV ( $E_{\text{iso}}/10^{52}$  ergs) $^{1/2}$  (Lamb et al. 2003b).